All-*trans* Retinoic Acid-Associated Low Molecular Weight Water-Soluble Chitosan Nanoparticles Based on Ion Complex

Dong-Gon Kim, Changyong Choi, Young-Il Jeong, Mi-Kyeong Jang, and Jae-Woon Nah*

Department of Polymer Science and Engineering, Sunchon National University, Jeonnam 540-742, Korea

Seong-Koo Kang

Research Instrument Center, Sunchon National University, Jeonnam 540-742, Korea

Moon-Soo Bang

Division of Chemical Engineering, Kongju National University, Cheonan 330-717, Korea

Abstract: The purpose of this study is to develop novel nanoparticles based on polyion complex formation between low molecular weight water-soluble chitosan (LMWSC) and all-*trans* retinoic acid (atRA). LMWSC nanoparticles encapsulating atRA based on polyion complex were prepared by mixing of atRA into LMWSC aqueous solution using ultrasonication. In FTIR spectra, the carbonyl group of atRA at 1690 cm^{-1} disappeared or decreased when ion complexes were formed between LMWSC and atRA. In ^{1}H NMR spectra, specific peaks of atRA disappeared when atRA-encapsulated LMWSC (RAC) nanoparticles were reconstituted into D_2O while specific peaks both of atRA and LMWSC appeared in D_2O/DMSO (1/3, v/v) mixture. XRD patterns also showed that the crystal peaks of atRA were disappeared by encapsulation into LMWSC nanoparticles. LMWSC nanoparticles encapsulating atRA have spherical shapes with particle size below 200 nm. The mechanism of encapsulation of atRA into LMWSC nanoparticles was thought to be an ion complex formation between LMWSC and atRA. LMWSC nanoparticles showed high atRA loading efficiency over 90% (w/w). AtRA was continuously released from nanoparticles over 10 days. In *in vitro* cell cytotoxicity test, free atRA showed higher cytotoxic effect against CT 26 colon carcinoma cell line on 1 day. However, RAC nanoparticles showed similar cytotoxicity against CT 26 cells on 2 day. These results suggest the potential for the introduction of LMWSC nanoparticles into various biomedical fields such as drug delivery.

Keywords: low molecular weight water-soluble chitosan, all-*trans* retinoic acid, polyion complex, nanoparticles, anticancer drug.

Introduction

Chitosan is a natural polymer derived from chitin by deacetylation. Since chitosan is regarded as biocompatible, biodegradable, and non-toxic, it is an interesting biomaterial because of its ability as a drug carrying materials and ease of modification.[1] Furthermore, chitosan has been reported to enhance drug delivery across the nasal or mucosal layer without damage.[2,3] Despite of its superiority as a biomaterial, chitosan is not fully soluble in water and then soluble in acidic solution. Aqueous solubility of chitosan only in acidic solution limits its application to bioactive agents such as gene delivery carriers, peptide carriers, and drug carriers. Recently, we developed water-soluble chitosan with low

molecular weight and free-amine group.[4,5] Low molecular weight water-soluble chitosan (LMWSC) is ease of soluble in neutral aqueous solution. Its advantage is ease of modification, useful as a gene or peptide drug carriers, and drug carriers.[6]

All-*trans* retinoic acid (atRA) is effective in the treatment of epithelial and hematological malignancies such as breast cancer, head and neck cancer, ovarian adenocarcinoma, and acute promyelocytic leukemia (APL).[7-9] However, some side effects such as retinoid acute resistance, hypertriglyceridermia, mucocutaneous dryness, and headache were reported in spite of its pronounced effects[10,11] limits the clinical applications of atRA. The cancer relapsed in any patients after a brief remission despite of continued atRA treatments, i.e., patients became resistant to further atRA treatment. It was reported that cancer recurrence might be due to the decrease of the plasma atRA concentration.[12] The rapid decrease of

*Corresponding Author. E-mail: jwnah@sunchon.ac.kr

half life of atRA with continuous oral administration or intravenous injection was reported by several authors.[13-15] Furthermore, very low aqueous solubility (0.1 μM at pH 7.3), photolability, and local-irritating reactions of atRA also limits its clinical application.[16,17]

It was reported that various kinds of formulation for atRA to overcome the side effects and rapid decrease of half-life. Giordano et al.[18] reported that atRA-loaded microspheres was effective in reducing the incidence of tractional retinal detachment by a sustained release of atRA. Liposome-encapsulated atRA showed higher longer serum tretinoin concentrations rather than oral atRA, resulting liposomal-atRA was effective to newly diagnosed acute promyelocytic leukemia (APL).[19] Solid lipid nanoparticles are reported to useful formulation to solve the poor aqueous solubility of atRA and able to use it by intravenous injection.[20] Choi et al.,[21] obtained the pseudo-zero-order release profiles of atRA for 5 weeks by encapsulating into biodegradable microspheres and control the release rate by the ratio of poly(L-lactide) (PLA) and PLA-poly(ethylene glycol) (PEG) block copolymer. Ezpeleta et al.,[22] reported that atRA was encapsulated into gliadin nanoparticles with high loading efficiency. An alternative approach would be to make complex between atRA into a positively charged carrier. Thunemann reported that polyethyleneimine (PEI) complexes with retinoic acid (RA) form nanoparticles for controlled release of atRA.[23] They showed a nanoparticulate complex between atRA and PEI has sizes ranging from 170 to 580 nm. In other reports,[24] they reported complexes between poly(ethylene oxide)-b-poly(L-lysine) and RA and formed core-shell type micelles.

For this study, we prepared atRA-encapsulated LMWSC (RAC) nanoparticles based on polyion complex formation between atRA and LMWSC. The physicochemical properties of RAC nanoparticles were investigated using various analytical equipments such as ^{1}H-NMR, TEM, X-RD, DLS, and fourier-transform infrared (FTIR) spectroscopy. Furthermore, atRA release test from nanoparticles and in vitro cytotoxicity against tumor cells were performed.

Experimental

Materials. Low molecular weight water-soluble chitosan (LMWSC) was obtained from KITTOLIFE Co. Korea. LMWSC was modified to enhance water-solubility as described previously as a water-soluble chitosan (M.W.= 10,000, deacetylation degree=96.3%).[4-6] All-trans retinoic acid (atRA), dimethylformamide (DMF), and dimethylsulfoxide (DMSO) were purchased from Sigma Co. Ltd. USA.

Preparation of atRA-Encapsulated LMWSC (RAC) Nanoparticles. 50 mg of LMWSC was dissolved in 10 mL of deionizer water (0.5%, w/v) without addition of acetic acid. AtRA dissolved in 1 mL of DMF was dropped into 10 mL of LMWSC solution (0.5%, w/v) with ultrasonica-

tion (probe type sonicator, Sonic & Materials Inc., Danbury, CT, USA) at an output power of 50 W for 10 cycles of 2 s on ice. After that, polyelectrolyte complexes of LMWSC and atRA were dialyzed against water 1 L × 6 for 9 h, i.e. 1 L of deionizer water was exchanged three times for 3 h and then exchanged three times for residual 6 h. Resulting solution was analyzed or lyophilized for 3 days. All procedure was performed on darkened condition.

To evaluate drug contents and loading efficiency, volume of dialyzed solution was adjusted to 25 mL with deionizer water and then 100 μL of solution was diluted with 10 mL of DMSO. LMWSC in distilled water (0.5% (w/w)) was used as a blank. Drug contents and loading efficiency of drug were estimated as following equation:

$$\text{Drug Contents} = \frac{\text{Amount of atRA in the Nanoparticles}}{\text{Weight of Nanoparticles}} \times 100$$

$$\frac{\text{Loading}}{\text{Efficiency}} = \frac{\text{Residual Amount of atRA in the Nanoparticles}}{\text{Feeding Amount of atRA}} \times 100$$

Particle Size and Zeta Potential Measurement. The particle size and zeta potential of RAC nanoparticles were investigated on dynamic light scattering (DLS) instrument. The DLS measurements were carried out using an ELS-8,000 electro phoretic LS spectrophotometer (Otsuka Electronics Co., Japan) equipped with a He-Ne laser operating at 632.8 nm at 25 °C and a fixed scattering angle 90°. A nanoparticle solution prepared by dialysis method was used for particle size measurement (concentration: 0.1 wt%) and measured without filtering.

Transmission Electron Microscope (TEM) Observation. RAC nanoparticles morphology was examined with a JEOL JEM-2000 FX-II transmission electron microscope (TEM). A drop of nanoparticles suspended in 0.01% of phosphotungstic acid was placed on a carbon film coated on a copper grid for TEM.

Fourier Transform-Infrared Spectroscopy Measurement. The chemical structure and complexes formation between LMWSC and atRA were analyzed by FTIR spectroscopy (Shimadzu, FTIR 8700, Japan). For measurement of FTIR, polyelectrolyte complexes between LMWSC and atRA were lyophilized for 3 days under dark condition. The KBr disc was prepared that RAC nanoparticles (3 mg) were mechanically blended with 300 mg of KBr for 10 min and the KBr disc obtained from 200 mg aliquot of the mixed powder was desiccated for 12 h at 60 °C under reduced pressure.

[1]H Nuclear Magnetic Resonance Spectra Study. ^{1}H NMR spectra of the RAC nanoparticles were recorded by Bruker spectrometer operating at 400 MHz. Chemical shifts (δ) were given in ppm using tetramethylsilan (TMS) as internal reference. ^{1}H NMR spectra were measured using DMSO

and D_2O. For ^1H NMR study, free atRA and LMWSC were dissolved in DMSO and D_2O, respectively. RAC nanoparticles were dissolved in D_2O and D_2O/ DMSO (1:3 v/v) mixture.

X-ray Diffractometer Measurement. X-ray powder diffractograms for RAC nanoparticles were recorded using a Rigaku D/MAX 1200 automated powder diffractometer with a rotating anode, a single-crystal monochromater, and a scintillator detector. $CuK\alpha$ radiation with a voltage of 40 kV and a current of 45 mA was obtained using a graphite monochromator. The wavelength λ was 1.541 Å. A typical $\theta/2\theta$ scan range was from $5°$ to $80°$. The plate-shaped sample was placed perpendicular to the incident X-rays ($\theta=90°$) on the electrically heated holder under a helium atmosphere.

AtRA Release from RAC Nanoparticles. AtRA release from nanoparticles was performed as follows: RAC nanoparticles were prepared as described above and volume of final aqueous solution was adjusted to 20 mL (i.e. 50 mg of polymer per 20 mL of water). Two mL of adjusted solution was diluted with 8 mL of phosphate buffered saline (PBS, pH7.4, 0.1 M) and introduced into dialysis tube (M.W. cutoff: 12,000). Dialysis tube containing nanoparticle solution was introduced into a bottle with 990 mL of PBS (PBS, 0.1 M, pH 7.4). Release test was performed at 37 °C with stirring rate of 100 rpm. The whole released medium was exchanged with fresh medium at predetermined time to maintain the sink condition. Released drug was measured at 365 nm with UV spectrophotometer (UV-1200, Shimadzu Co., Ltd. Japan) and calculated as a cumulative value. LMWSC itself was used as a blank.

For release test of free atRA, 20 mg of atRA was dissolved in 1 mL of DMSO. 25 μL of this solution was diluted with 10 mL of PBS (pH 7.4, 0.1 M). After that, diluted solution was introduced into dialysis tube. Dialysis tube was introduced into a bottle with 990 mL of PBS (PBS, 0.1 M, pH 7.4). Following procedures were performed similar to nanoparticle release test. All procedures are protected from light.

***In vitro* Cell Cytotoxicity Test.** CT-26 colon carcinoma cells were incubated in Dulbeco's modified eagles medium (DMEM) supplemented with 10% (w/w) FBS at CO_2 incubator (5% CO_2, 37 °C). 5×10^3 cells of CT-26 at exponential phase were inoculated into 96 well plate. For cell cytotoxicity of free atRA, 20 mg of atRA were dissolved in DMSO and diluted with PBS. Nanoparticles sterilized with 0.45 μm syringe filter and diluted with PBS. Diluted free atRA and nanoparticles were added into 96 well plates. For control, 0.5% (v/v) of DMSO in PBS was treated. For placebo, 10 mg LMWSC was dissolved in 5 mL of deionizer water and then components of PBS were added. 1 N NaOH was used to adjust pH to 7.4. LMWSC solution was diluted with PBS and sterilized with 0.2 μm syringe filter. Sterilized LMWSC solution was added into 96 well plates.
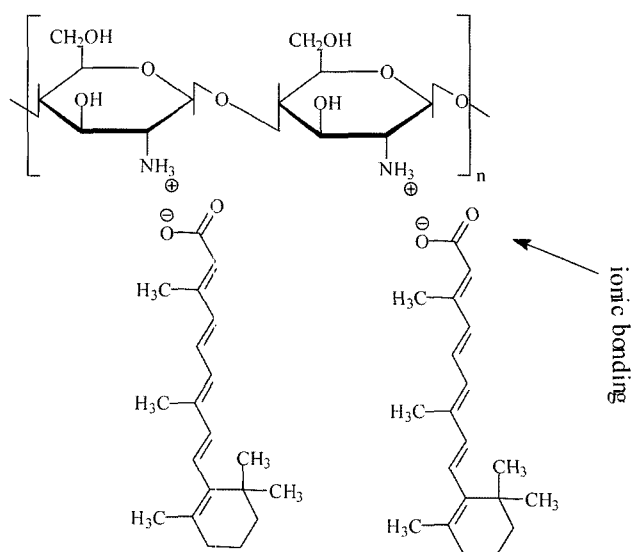

Figure 1. Scheme of nanoparticle formation based on polyelectrolytes complexes of LMWSC and atRA.

Results

Characterization of LMWSC Nanoparticles. LMWSC nanoparticles encapsulated atRA must be formed by ion complexes between the amine group of LMWSC and the carboxyl group of atRA[23] as shown in Figure 1. The morphology of RAC-5 nanoparticles is shown in Figure 2. As shown in Figure 2, atRA-LMWSC complexes have spherical shapes with particle size of < 200 nm. Table I shows the results of formation of atRA-LMWSC complexes. The feeding amount of atRA at the beginning of complexes formation was 2, 5, 10 mg, and the LMWSC solution was 0.5% (w/v) as shown in Table I. Encapsulation efficiency was higher than 90% (w/w) at all formulation. Particle sizes of RAC nanoparticles were increased according to the increased feeding amount of drug.

Figure 3 shows FTIR spectra of atRA, LMWSC, and RAC nanoparticles. As shown in Figure 3, the spectra of atRA itself and ion complexes between LMWSC and atRA were characterized at around 1255 cm^{-1}. AtRA itself has specific (C-O stretch vibration) absorbance around 1255 cm^{-1} and the significant decrease in the absorbance was observed according to the complex formation between LMWSC and atRA. Also, carbonyl group of atRA characterized around 1690 cm^{-1} disappeared or decreased when ion complexes were formed between LMWSC and atRA. Interestingly, the increased drug contents induce increased absorbance (1690 cm^{-1}), suggesting that the increase of absorbance reflects the uncomplexed or aggregated atRA in the complexes formulation.[25]

Figure 4 shows ^1H-NMR spectra of RAC-5 nanoparticles. As shown in Figure 4, atRA and LMWSC itself showed their specific peak characteristics. When RAC nanoparticles were reconstituted into D_2O, specific peaks of atRA disap-

Table I. Characterization of RAC Nanoparticles

Sample	LMWSC (%, w/v)	atRA (mg)	Drug Contents (%, w/w)	Loading Efficiency (%, w/w)	Particle Size (nm)	Zeta Potential (mV)
LMWSC 2	0.5	2	3.7	95.1	102.7 ± 37.2	64.1
LMWSC 5	0.5	5	8.5	93.2	139.7 ± 44.9	63.5
LMWSC 10	0.5	10	15.4	91.2	202.3 ± 55.5	62.6

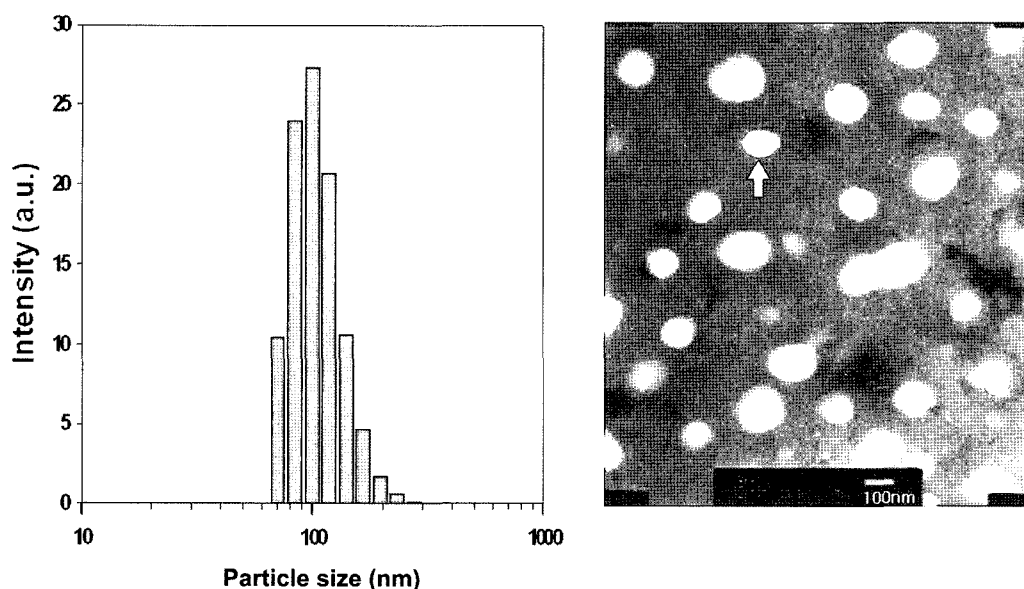*Basic preparation conditions are described in materials and methods.

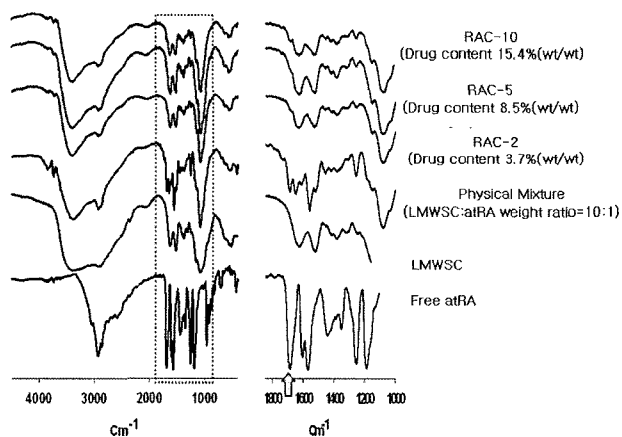Figure 2. TEM photograph of nanoparticles (RAC-5).

Figure 3. FTIR spectroscopy of RAC nanoparticles.

Figure 4. ¹H NMR spectra of RAC nanoparticle in D₂O/DMSO mixtures (1:4, v/v) (a), D₂O (b), free atRA in DMSO (c), and LMWSC in D₂O (d).

peared at their proton spectra while a specific peak of LMWSC was shown. However, specific peaks of both of atRA and LMWSC appeared when RAC nanoparticles were dissolved into D₂O/DMSO((1/3, v/v) mixtures. These results indicated that atRA was encapsulated in the core of the RAC nanoparticles when nanoparticles were reconstituted
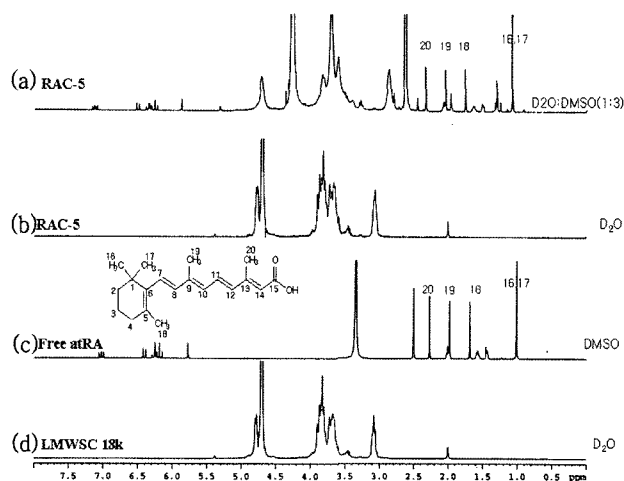
in water but RAC nanoparticles were destroyed at D₂O/ DMSO (1:3, v/v) and specific peaks both of atRA and LMWSC were shown at their proton spectra. These results

indicated that atRA encapsulated in the core of the RAC nanoparticles did not liberated from the RAC nanoparticles due to the ion complexes between carbonyl group of atRA and amine group of chitosan.

Figure 5 shows XRD pattern of atRA and RAC nanoparticles. AtRA showed sharp specific crystalline peaks whereas LMWSC itself showed broad peaks. Sharp crystalline peaks
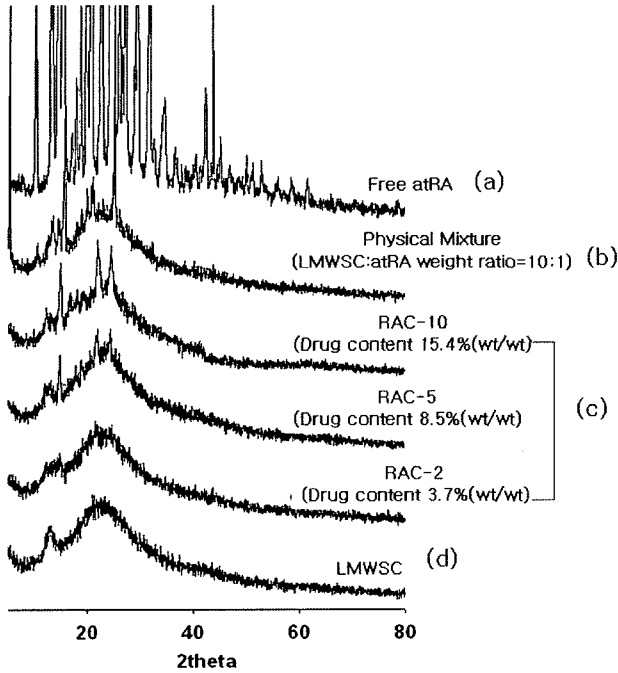
of atRA disappeared when ion complexes are formed at RAC nanoparticles. However, specific crystalline peaks of atRA were remained at physical mixtures of atRA and LMWSC (weight ratio of chitosan:atRA = 10:1).

Drug Release from RAC Nanoparticles. Figure 6 shows the atRA release from RAC nanoparticles. As shown in Figure 6, drug releases continued over 10 days whereas release of free atRA dialysis bag were finished for 2 days. The higher the drug contents showed the slower the release rate of drug. These results indicated that the hydrophobic drug was released very slowly, and that it can be crystallized at higher

Figure 5. X-ray powder diffraction patterns of atRA-encapsulated chitosan nanoparticles. AtRA (a), atRA/chitosan physical mixture (atRA:chitosan weight ratio = 1:10) (b), RAC nanoparticles (RAC-10,5,2) (c), and LMWSC (d).
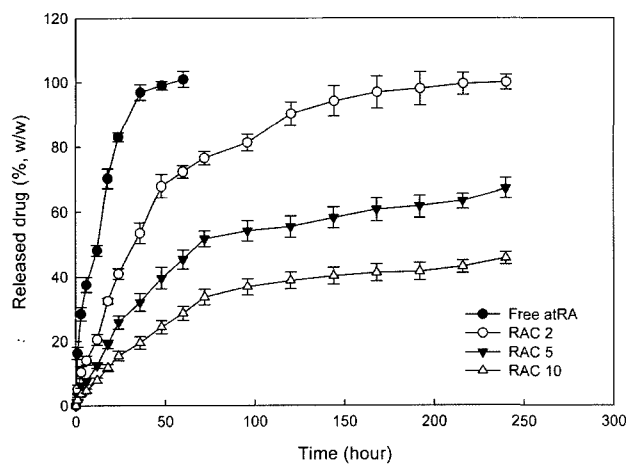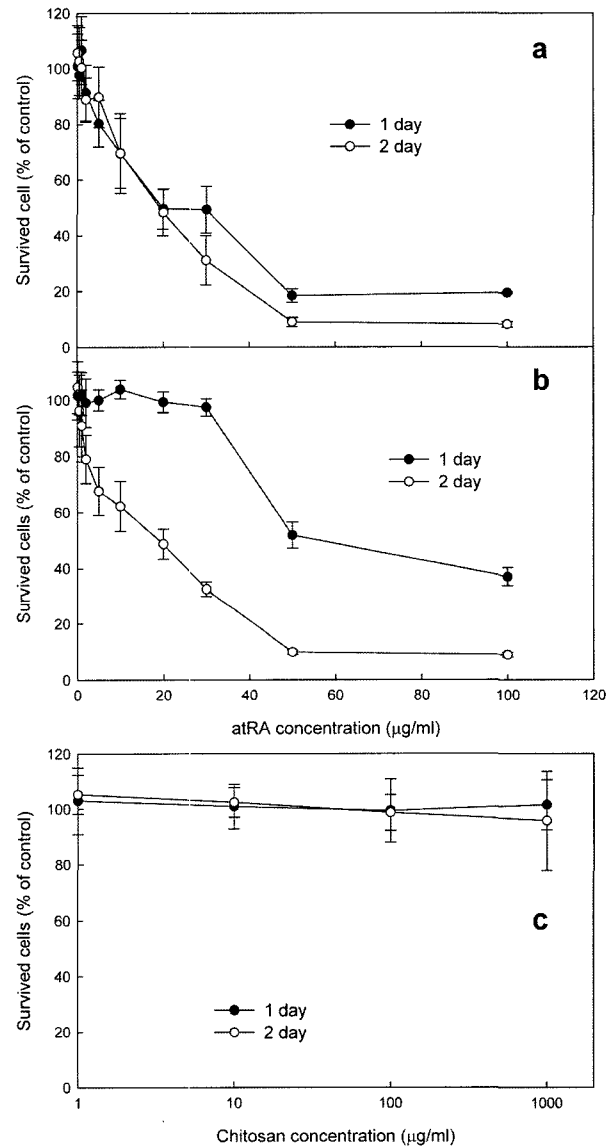

Figure 6. The release profiles of atRA from atRA-encapsulated chitosan nanoparticles. The data represents mean ± standard deviations (n=3).

Figure 7. Cell cytotoxicity of atRA-encapsulated chitosan nanoparticles against CT-26 colon carcinoma cell lines. CT 26 (5 × 10³ cells/well) were treated with atRA (a), atRA-encapsulated chitosan nanoparticles (b), and chitosan (c). 0.5% (v/v) DMSO were treated for control (mean ± s.d., n=8).

drug loading in the core of the vehicles since atRA is practically a water-insoluble drug.

Tumor Cell Cytotoxicity of RAC Nanoparticles. In *in vitro* cell cytotoxicity test (Figure 7), free atRA was showed higher cytotoxic effect against CT 26 colon carcinoma cell line on 1 day. RAC nanoparticles and free atRA showed similar cytotoxicity against CT 26 cells on 2 day. At 2 day of treatment, only below 10% of tumor cells are remained at 50 μg/mL equivalent concentration of atRA. It suggested that chitosan itself does not affect on the cell viability up to 1 mg/mL of LMWSC concentration.

Discussion

Since atRA is one of the highly hydrophobic and photo-sensitive drugs, complexation with water-soluble materials such as polylysine, PEI, or chitosan is thought to be an ideal approach to solve the solubility and photo-stability problem.[6,23,24] Among various kinds of encapsulation or formulation, complexes formation using cationic polymer should be a promising procedure to solve the solubility and stability problems of atRA due to anionic characteristics. We had reported a water-soluble chitosan with high contents of free-amine group in the main chain elsewhere.[4,5] Low molecular water-soluble chitosan with high density of free-amine group is distinguished in water-solubility, i.e., normal chitosan does not completely soluble in water and required acidic solution to dissolve it. These properties have great potentials of applications in the drug delivery system and biomedical applications since most of the drugs, proteins, peptides, and DNA drugs are sensitive to acidic solution and easy to inactivate in the high acidic environment. Practically, we had shown that low molecular water-soluble chitosan is a good candidate for the gene delivery system with a high transfection efficiency.[6] From these findings, low molecular water-soluble chitosan is thought to be a good candidate for atRA. Thunemann[23,24] reported already basic concept about ion complex between atRA and cationic polymer such as PEI or poly(L-lysine) (PLL). They showed a nanoparticulate complex between atRA and PEI has sizes ranging from 170 to 580 nm.[23] In other reports,[24] they reported complexes between poly(ethylene oxide)-*b*-PLL and atRA and formed core-shell type micelles. However, PLL and PEI are known to cytotoxic and PEI is not degradable at biological system. Other types of drug carriers based on ion complex formation between cationic drug and anionic polymer were reported by Kataoka group.[26,27] They reported that ciplatin incorporated polymeric micelle showed superior incorporation efficiency and antitumor ability.

LMWSC nanoparticles encapsulating atRA were prepared by mixing of atRA (dissolved in DMF) into the chitosan aqueous solution with ultrasonication following dialysis procedure. It suggested that formation mechanism of LMWSC nanoparticle and atRA encapsulation is based on ion complex formation between amine groups of chitosan and carboxyl group of atRA[23] as shown in Figure 1. Practically, spherical nanoparticles were observed with TEM. FTIR results supported that complex formation of atRA and LMWSC, i.e. peaks of C-O stretch (1255 cm^{-1}) and carbonyl group (around 1690 cm^{-1}) were decreased at LMWSC nanoparticles as shown in Figure 4. Similar results were also reported by Thunemann *et al.*[23] They reported that specific peaks were decreased or disappeared when ion complex was formed between PEI and atRA. Specific peaks of atRA and LMWSC were increased according to drug release from nanoparticles.

RAC nanoparticles have particle sizes below 200 nm. It was reported that other kinds atRA formulation have particles sizes larger than 200 nm.[20-24] Complexes below 200 nm are more acceptable for intravenous injection and site-specific targeting.[28] Loading efficiency of atRA was higher than 90% (w/w) at all formulations. We suggested that these results are noticeable since LMWSC complexes are a good candidate for high drug loading efficiencies with small particle size. Most of the other reports showed bigger particle size with high atRA loading.[20-22] Choi *et al.*[21] reported that high efficiency of drug loading over 90% (w/w) is obtained into the microspheres, but their particles have several micrometers in particle size. Several micrometers in particle size are not acceptable for intravenous injection. Gliadin nanoparticles also have a high entrapment efficiency of about 75% (w/w), but their particle sizes are about 500 nm.[22] Lim *et al.*[20] reported that atRA-entrapped solid lipid nanoparticles are below 200 nm in particle size, but their nanoparticles have very low drug contents.

Drug release from RAC nanoparticles is slower than we expected. As shown in Figure 6, drug releases continued over 10 days. It was thought that dialysis bag itself also act as a barrier at drug diffusion as shown in Figure 6. At higher drug contents the release rate of drug was very slow. These results indicated that the hydrophobic drug was released very slowly, and that it can be crystallized at higher drug loading in the core of the vehicles[26] since atRA is practically a water-insoluble drug. At this moment, atRA might be crystallized in the nanoparticle core. Crystallized drug can be dissolved and/or decomplexed slowly owing to their hydrophobic properties. In cell cytotoxicity test, RAC nanoparticles showed similar cytotoxicity to free atRA at 2 day of treatment. It was thought that RAC nanoparticles does uptake by tumor cells directly rather than released drug uptake by cells because drug release from LMWSC nanoparticles were very slow. We will report mechanism of action of LMWSC nanoparticle on the tumor cell cytotoxicity in another report.

We suggest that our low molecular water-soluble chitosan is superior candidate to formulate and store atRA as a nanoparticle form. Lim *et al.*[29] also reported that the chemical stability of atRA was substantially improved by incorporation in solid lipid nanoparticle powder, i.e. 90% (w/w) of intact

atRA remained after 3 month.

Conclusions

Novel types of nanoparticles based on polyion complex formation between LMWSC and atRA were developed. LMWSC nanoparticles encapsulating atRA based on polyion complex prepared by mixing of atRA into LMWSC aqueous solution using ultrasonication. At FTIR spectra, carbonyl group of atRA characterized around 1690 cm^{-1} disappeared or decreased when ion complexes were formed between LMWSC and atRA. At ^{1}H NMR spectra, specific peaks of atRA disappeared when RAC nanoparticles were reconstituted into D$_2$O while specific peaks both of atRA and LMWSC appeared at D$_2$O/DMSO (1/3, v/v) mixture. XRD patterns also showed that crystal peaks of atRA disappeared by encapsulation into RAC nanoparticles. LMWSC nanoparticles encapsulating atRA have spherical shapes with particle size below 200 nm. The mechanism of encapsulation of atRA into LMWSC nanoparticles thought to be an ion complex formation between LMWSC and atRA. LMWSC nanoparticles showed high atRA loading efficiency over 90% (w/w). AtRA was continuously released from nanoparticles over 2 week. In *in vitro* cell cytotoxicity test, free atRA showed higher cytotoxic effect against CT 26 colon carcinoma cell line on 1 day. However, LMWSC nanoparticles showed similar cytotoxicity against CT 26 cells on 2 day. Based on these results, it is possible to introduction of the LMWSC nanoparticles into various biomedical fields such as drug delivery.

References

(1) S. Hirano, *Polym. Int.*, **48**, 732 (1999).

(2) R. Fernandez-Urrusuno, P. Calvo, C. Remunan-Lopez, J. L. Vila-Jato, and M. J. Alonso, *Pharm. Res.*, **16**, 1576 (1999).

(3) A. F. Kotez, B. J. de Leeuw, H. L. Lueben, A. G. deBoer, J. C. Verhoef, and H. E. Junginger, *Int. J. Pharm.*, **159**, 243 (1997).

(4) M. K. Jang, Y. I. Jeong, C. S. Cho, S. H. Yang, Y. E. Kang, and J. W. Nah, *Bull. Korean Chem. Soc.*, **23**, 914 (2002).

(5) J. W. Nah and M. K. Jang, *J. Polym. Sci.; Part A: Polym. Chem.*, **40**, 3796 (2002).

(6) M. Lee, J. W. Nah, Y. Kwon, J. J. Koh, K. S. Ko, and S. W. Kim, *Pharm Res.*, **18**, 427 (2001).

(7) F. Giannini, R. Maestro, T. Vukosa, T. Vljevic, F. Pomponi, and M. Boiocchi, *Int. J. Cancer*, **70**, 194 (1997).

(8) G. Krupitza, W. Hulla, H. Harant, E. Dittrich, E. Kallay, and H. Huber, *Int. J. Cancer*, **61**, 649 (1995).

(9) E. J. Huang, Y. C. Ye, S. R. Chen, J. R. Chai, J. X. Lu, L. Zhoa, L. J. Gu, and Z. Y. Wang, *Blood*, **72**, 567 (1988).

(10) B.A. Conley, M. J. Egorin, R. Sridaha, R. Finley, R. Hemady, S. Wu, N. S. Tait, D. A. Van Echo, and D. A. Van Echo, *Cancer Chem. Pharm.*, **39**, 291 (1997).

(11) S. R. Frankel, A. Eardley, G. Lauwers, M. Weiss, and R. P. Warrell, *Ann. Intern. Med.*, **117**, 292 (1992).

(12) J. R. F. Muindi, S. R. Frankel, W. H. Miller, A. Jakubowski, D. A. Scheinberg, C. W. Young, E. Dmitrovsky, and R. P. Warrell, *Blood*, **79**, 299 (1992).

(13) C. C. Achkar, J. M. Bentel, J. F. Boylan, H. I. Scher, L. J. Gudas, and W. H. Miller, *Drug Metab. Disp.*, **22**, 451 (1994).

(14) T. Hirota, T. Fujimoto, K. Konno, Y. Sakakibara, N. Katano, M. Tsurusawa, K. Takitani, and M. Miyake, *Jap. J. Clin. Hemat.*, **38**, 1170 (1997).

(15) R. S. Shelly, H. W. Jun, J. C. Price, and D. E. Cadwallader *J. Pharm. Sci.*, **71**, 904 (1982).

(16) P. A. Lehman, J. T. Slattery, and T. J. Franz, *Percutaneous J. Invest. Dermatol.*, **91**, 56 (1988).

(17) E. Z. Szuts and F. I. Harosi, *Arch. Biochem. Biophys.*, **287**, 297 (1991).

(18) G. G. Giordano, M. F. Refojo, and M. H. Arroyo, *Invest. Ophtal. Vis. Sci.*, **34**, 2743 (1993).

(19) E. H. Estey, F. J. Giles, H. Kantarjian, S. O'Brien, J. Cortes, E. J. Freireich, G. Lopez-Berestein, and M. Keating, *Clin. Observ. Interv. Ther.*, **94**, 2230 (1999).

(20) S. J. Lim and C. K. Kim, *Int. J. Pharm.*, **243**, 135 (2002).

(21) Y. Choi, S. Y. Kim, S. H. Kim, K. S. Lee, C. Kim, and Y. Byun, *Int. J. Pharm.*, **215**, 67 (2001).

(22) I. Ezpeleta, J. M. Irache, S. Stainmesse, C. Chabenat, J. Gueguen, Y. Popineau, and A. M. Orecchioni, *Int. J. Pharm.*, **131**, 191 (1996).

(23) A. F. Thünemann and J. Beyermann, *Macromolecules*, **33**, 6878 (2000).

(24) A. F. Thünemann, J. Beyermann, and H. Kukula, *Macromolecules*, **33**, 5906 (2000).

(25) N. L. Rockley, B. A. Halley, M. G. Rockley, and E. C. Nelson, *Anal Biochem*, **133**, 314 (1983).

(26) N. Nishiyama and K. Kataoka, *J. Control Release*, **74**, 83 (2001).

(27) N. Nishiyama, S. Okazaki, H. Cabral, M. Miyamoto, Y. Kato, Y. Sugiyama, K. Nishio, Y. Matsumura, and K. Kataoka, *Cancer Res.*, **63**, 8977 (2003).

(28) R. Gref, Y. Minamitake, M. T. Peracchia, V. Trubetskoy, V. Torchilin, and R. Langer, *Science*, **18**, 1600 (1994).

(29) S. J. Lim, M. K. Lee, and C. K. Kim, *J. Control Release*, **100**, 53 (2004).